

Chapter 7 Semiconductor Detectors

7.1. Introduction

Semiconductor detectors are most commonly used when best energy resolution is intended. As discussed in the previous chapters, each type of radiation detector produces its inherent output product after interaction with radiation. In semiconductor detectors, the fundamental information carriers are electron-hole pairs, which are produced along the path taken by the charged particle (primary or secondary) through the detector. By collecting electron-hole pairs, the detection signal is formed.

Of the available semiconductor materials, silicon is mainly used for charged particle detectors and soft X-ray detectors while germanium is widely used for gamma-ray spectroscopy.

7.2. Semiconductor Property

Band structure in solid

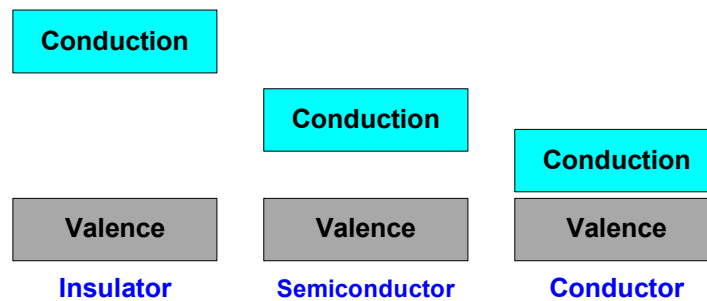


Fig. 7.1. Band structure for electron energies in solids.

In a metal, the highest occupied energy band is not completely full and electrons can easily migrate. In an insulator or semiconductor, electrons must obtain energy so that they cross the band gap to reach the conduction band and the conductivity is much lower.

Insulators have a larger band gap, therefore more energy is required to excite valence electrons to the conduction band. The band gap is ~ 1 eV for semiconductor materials while it is greater than 5 eV for insulator materials.

The excitation of an electron to the conduction band creates a vacancy in the valence band. Then, an electron-hole pair is formed.

The probability per unit time that an electron-hole pair is thermally generated is

$$P(T) = CT^{3/2} \exp(-E_g/2kT)$$

Where T is absolute temperature, E_g is the band gap energy, K is the Boltzmann constant and C is a proportionality constant characteristic of the material.

Thermal excitation in semiconductor materials is strongly dependent on temperature. A pure semiconductor is an insulator at absolute zero. As the temperature increases electrons can be thermally excited from the valence band to the conduction band.

Ideal radiation detectors should have no charge in the absence of radiation (and lots of charge in the presence of an ionizing radiation event). This is one of the reasons why some semiconductor detectors are cooled with liquid nitrogen (~ 77 K). Cooling reduces the number of electron-hole pairs in the crystal.

Migration of charge carriers in an applied electric field

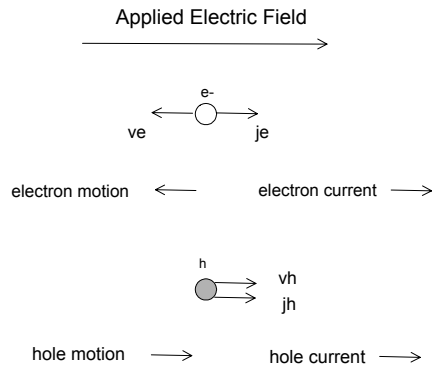


Fig. 7.2. Motions of electron and hole in an applied electric field.

If an electric field is applied to semiconductor material, both the electrons and holes undergo net migration. The electrons and holes migrate in opposite directions but this results in a net current in the same direction.

Intrinsic and doped semiconductors

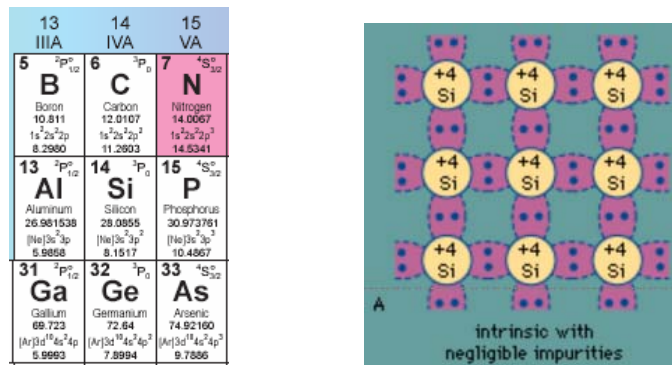


Fig. 7.3. Covalent bond of the intrinsic semiconductor material.

Intrinsic semiconductors are completely pure semiconductors where all the electrons in the conduction band and all the holes in the valence band are caused by thermal excitation (in the absence of ionizing radiation).

This means that the number of electrons in the conduction band equals the number of holes in the valence band.

However, intrinsic semiconductors are extremely difficult to achieve in practice because very low levels of impurity affect the electrical properties of a semiconductor. Small levels of residual impurities will dominate the properties of a semiconductor.

Semiconductor materials are therefore often doped with other materials to change their characteristics.

N-type semiconductor

The example used here is silicon, but similar arguments hold for other semiconductors. Silicon is a tetravalent element, the normal crystal structure is 4 covalent bonds.

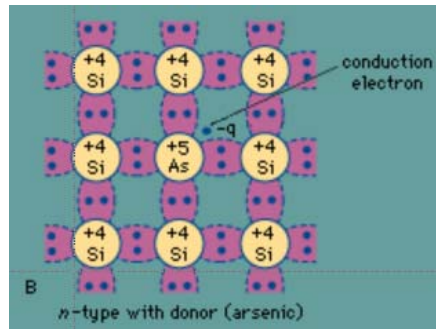
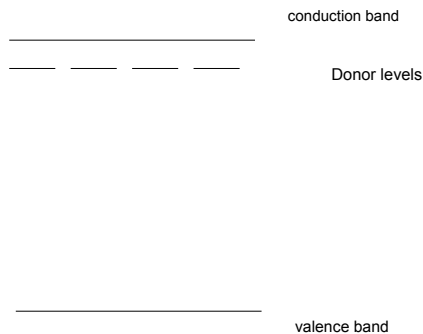


Fig. 7.4. Effect of an n-type impurity on the lattice structure.

When silicon is doped with a pentavalent element, Group V in the periodic table, it becomes an n-type semiconductor.

The element (P in this example) has one electron left over after the covalent bonds are formed; this donor electron is donated to the conduction band.



The extra electrons occupy levels in the normally forbidden band, and very little energy is required to excite them into the conduction band. Thermal excitation will excite electrons into the conduction band even at low temperatures.

Fig. 7.5. Donor energy level.

The conduction electrons are completely dominated by the number of donor sites. The number of conduction electrons contributed by silicon is small.

The number of conduction electrons, $n \approx N_D$, number of donor sites.

Charge neutrality is maintained because ionized donor sites balance the conduction electrons. **These sites are not holes because they cannot move.** The net result is that the number of conduction electrons is increased, while the number of holes is reduced.

P-type semiconductor

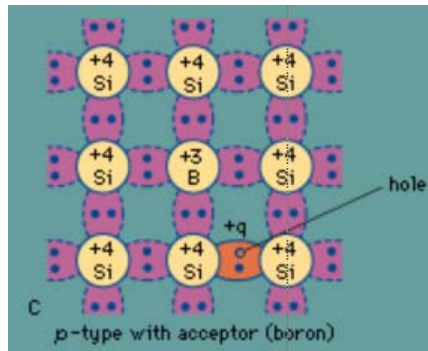
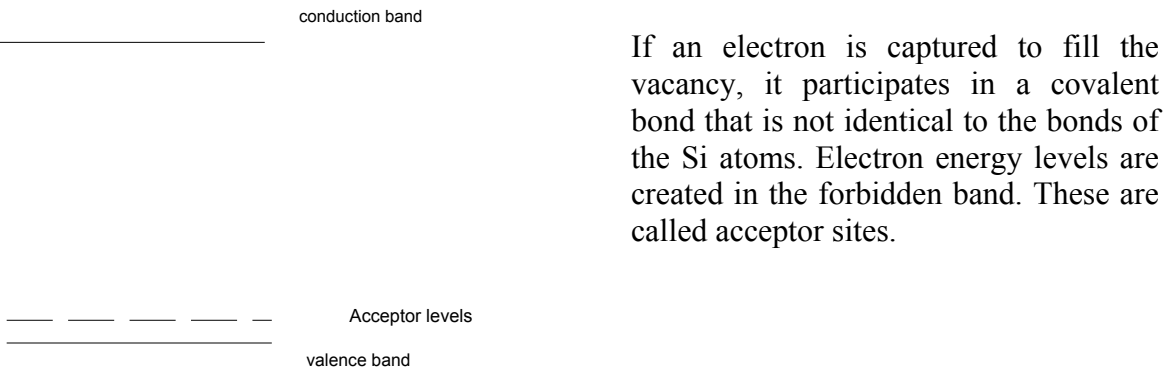


Fig. 7.6. Effect of a p-type impurity on the lattice structure.

When silicon is doped with a trivalent element such as boron, one covalent bond is left unsaturated because there are three valence electrons but four covalent bonds. The vacancy represents a hole, similar to that left behind when a normal valence electron is excited to the conduction band. However the energy structure is modified.



If an electron is captured to fill the vacancy, it participates in a covalent bond that is not identical to the bonds of the Si atoms. Electron energy levels are created in the forbidden band. These are called acceptor sites.

Fig. 7.7. Acceptor energy level.

Holes are created in the valence band for approximately every acceptor impurity added, because the acceptor sites are preferentially filled.

The number of acceptor sites dominates the number of holes.

Therefore, **the number of holes, $p \approx N_A$, the number of acceptor sites.**

The number of holes is increased, reducing the number of conduction electrons.

7.3. Action of radiation in semiconductors

Average energy per electron-hole pair (w-value)

The fundamental information associated with the interaction between a semiconductor detector and radiation is contained in the electron-hole pairs created. The number of electron-hole pairs is governed by the average energy spent by the charged particle to produce a single electron-hole pair. This quantity is much larger than the bandgap as shown in the table. It is largely independent of both the energy and type of the incident radiation, which simplifies estimation of the electron-hole pairs if the energy deposited by radiation is available. The energy per pair is ~ 3 eV, which is smaller than w-values of gas-filled detectors by a factor 10.

	Bandgap		Energy per electron-hole pair	
	300 K	0 K	300 K	77 K
Si	1.11	1.16	3.62	3.76
Ge	0.66	0.74		2.96

The doping levels in p- or n-type semiconductors are usually low and radiation interactions with these impurity elements can be neglected. Therefore, p-type or n-type silicon of equal thickness will show same interaction pattern with radiation.

Fano factor

In addition to the mean number, the variance in the number of charge carriers is also important for energy resolution. It is not unusual that the actual variance significantly deviates from the value expected if the formation of the charge carriers were governed by the Poisson distribution. The Fano factor is defined as

$$F = \text{observed variance} / \text{variance from Poisson model}$$

7.4. Semiconductor junction

A. Basic junction properties

To collect charge carriers (electron-hole pairs) in a semiconductor detector produced through radiation interaction, an electric field must exist as in the case of gas-filled detectors. The applied high voltage varies depending on the detector size and is typically hundreds or thousands of volts. This high voltage induces leakage current even in the absence of radiation because the semiconductor material itself has a finite conductivity.

If a 1 mm thick bulk silicon semiconductor with a 1 cm^2 area is used for radiation detection and a 500 V high voltage bias is applied, the leakage current through the silicon will be ~ 0.1 A from the resistivity of the high purity silicon ($\sim 50,000 \text{ } \Omega\text{-cm}$). However, an impulse current level produced by radiation interaction is $\sim \mu\text{A}$, which is significantly lower than the leakage current. Therefore an active method, a p-n junction, is required to reduce the leakage current to pickup the signal corresponding to the radiation interaction. In other word, semiconductor detectors are a “sandwich” of p- and n-type materials; the detector is a semiconductor diode.

The standard process of making a junction is to modify the impurity concentration of one side of the material so that both sides can have opposite configurations. Depending on the type of the initial material, two different configurations are possible as shown in Fig. 7.8.

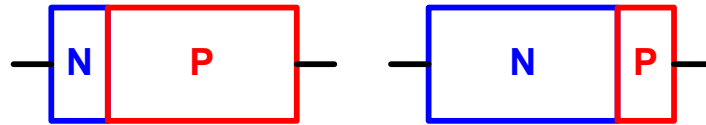


Fig. 7.8. P-n junction.

If the initial material was p-type, the majority of radiation interactions are in the p-type material, so this is called a p-type detector. Similarly, the majority of interactions are in the n-type material in the second case, hence called an n-type detector.

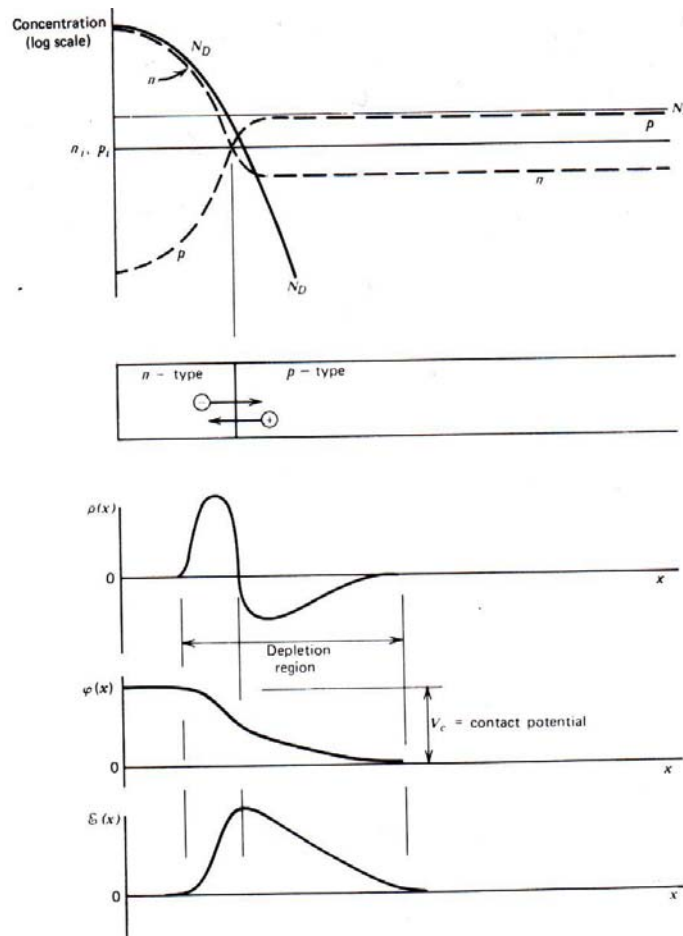


Fig. 7.9. The assumed concentration profiles for the p-n junction and the corresponding profiles for the space charge, electric potential and electric field.

An example of the p-n junction and its effect is illustrated in Fig. 7.9. The process of the junction begins with a p-type crystal in this case. The original acceptor concentration N_A is shown as a constant level. When an n-type impurity diffuses into the crystal from the left side, the donor impurity concentration N_D is produced. Near the surface, N_D can be made to exceed the acceptor concentration, which leads to conversion of the left side of the crystal into n-type material. Then,

In the n-type region, there is a much higher density of conduction electrons.

In the p-type region, there is a much lower density of conduction electrons.

The junction represents a **discontinuity in electron density**, and a net diffusion from the high density side to low density takes place for both electrons and holes.

The effect of the diffusion from each side of the junction is to build up a net negative space charge on the p-type side and a net positive space charge on the n-type side of the junction, as compared to the rest of the p-type.

The accumulated space charge creates an electric field that diminishes the tendency for further diffusion. At equilibrium, the field is just adequate to prevent additional diffusion across the junction and a steady state charge distribution is established. The region over which the imbalance is established is called the **depletion region**.

The buildup of net charge within the region of the junction creates an electric potential across the junction. The value of the potential V at any point can be found by solution of Poisson's equation:

$$\nabla^2 V = -\frac{\rho}{\epsilon}$$

where ρ is the net charge density and ϵ is the dielectric constant. In one dimension

$$\frac{d^2 V(x)}{dx^2} = -\frac{\rho(x)}{\epsilon}$$

The graphical example was shown in the figure. At equilibrium, the potential difference across the junction, **contact potential**, is equivalent to the full bandgap value. The corresponding electric field is

$$\vec{E} = -\nabla V$$

Thus, the direction of the electric field is such that it opposes further diffusion of electrons and holes.

The depletion region will function as a radiation detector (although with relatively poor performance.) The electric field sweeps electrons created in or near the junction

back toward the n-type material, and any holes are swept back toward the p-type material; the motion of these electrons and holes creates the electric signal.

However, the contact potential is too low to generate electric fields that will move charge carriers quickly. Incomplete charge collection can result, as charges have time to be trapped or recombine. This means that the noise characteristics of an unbiased junction are poor. Moreover, **the thickness of the depletion region is quite small**, so that only a small volume of the crystal acts as a radiation detector, which **requires extension of the depletion region**.

B. Reverse biasing

The semiconductor detector operates much better as a radiation detector if an external voltage is applied across the junction in the reverse biased direction.

The semiconductor junction or semiconductor detector is really a large diode. The junction is reverse-biased when the p-side of the junction is made negative with respect to the n-side. The natural potential difference that arises upon contact of the two sides of the junction is greatly enhanced. The minority carriers are attracted across the junction, but because their concentration is low, the reverse current across the junction is pretty small. The p-n junction acts as a rectifying element i.e. it allows relatively free flow of current in one direction, while representing a large resistance to current flow in the other direction.

Reverse biasing a junction increases the thickness of the depletion region because the potential difference across the junction is enhanced.

We can use the following simplified model of charge distribution to describe the properties of the reverse bias junction.

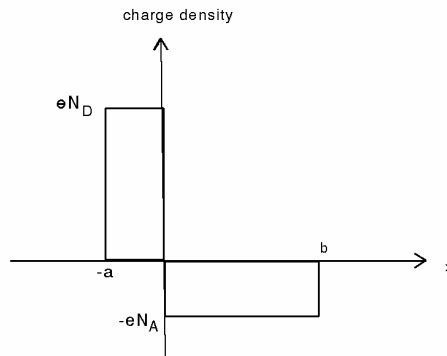


Fig. 7.10. Distribution of space charges across the p-n junction.

In this idealized distribution,

$$\rho(x) = eN_D \quad (-a \leq x < 0) :$$

Electron diffusion results in a uniform positive space charge between $-a$ and 0 .

$$\rho(x) = -eN_A \quad (0 \leq x \leq b):$$

Hole diffusion results in a uniform negative space charge between 0 and b.

The net charge is zero: $N_D \times a = N_A \times b$

The electrical potential can be found from solution of

$$\frac{d^2V(x)}{dx^2} = -\frac{\rho(x)}{\epsilon}$$

where in this case

$$\frac{d^2V(x)}{dx^2} = -\frac{\rho(x)}{\epsilon} = -\frac{eN_D}{\epsilon} \quad (-a \leq x < 0)$$

$$\frac{d^2V(x)}{dx^2} = -\frac{\rho(x)}{\epsilon} = +\frac{eN_A}{\epsilon} \quad (0 \leq x \leq b)$$

The electrical field $\vec{E} = -\nabla V$ must be 0 at the edges of the charge distribution, i.e.

$$\frac{dV}{dx}(x = -a) = 0 \quad \text{and} \quad \frac{dV}{dx}(x = b) = 0$$

Integrating the differential equations:

$$\frac{dV(x)}{dx} = -\frac{eN_D}{\epsilon}(x+a) \quad (-a \leq x < 0)$$

$$\frac{dV(x)}{dx} = \frac{eN_A}{\epsilon}(x-b) \quad (0 \leq x \leq b)$$

The difference in potential across the junction is V_0 , the applied voltage. (The contact potential is so much less than the applied voltage that it can be ignored).

Therefore, applying $V(-a) = V_0$ and $V(b) = 0$

And integrate again to obtain $V(x)$

$$V(x) = -\frac{eN_D}{2\epsilon}(x+a)^2 + V_0 \quad (-a \leq x < 0)$$

$$V(x) = \frac{eN_A}{2\epsilon}(x-b)^2 \quad (0 \leq x \leq b)$$

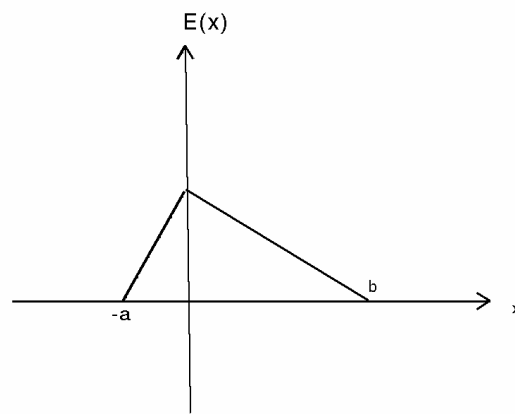


Fig. 7.11. Electric field across the p-n junction.

The solutions match at $x=0$ therefore

$$-\frac{eN_D a^2}{2\epsilon} + V_0 = \frac{eN_A b^2}{2\epsilon} \Rightarrow N_A b^2 + N_D a^2 = \frac{2\epsilon V_0}{e}$$

And since $N_D \times a = N_A \times b$, the above equation becomes

$$N_A b(a+b) = \frac{2\epsilon V_0}{e}$$

If we define d as the total width of the depletion region,

$$d = a + b$$

Since the n-side doping level is much higher, $N_D \gg N_A$, and using the relation $N_D \times a = N_A \times b$, the total width of the depletion region d is determined by

$$d = a + b \cong b = \left(\frac{2\epsilon V_0}{eN_A}\right)^{1/2}$$

A generalized solution for the depletion width (or depth) is

$$d \cong \left(\frac{2\epsilon V_0}{eN}\right)^{1/2}$$

where, N represents the net impurity concentration on the initial semiconductor material. Thus, the size of the depletion region depends on both bias voltage and the initial impurity concentration.

The depletion region behaves as a capacitor since the charges are built up on either side of the p-n junction. The capacitance per unit area is

$$C = \frac{\epsilon}{d} \cong \left(\frac{e\epsilon N}{2V_0}\right)^{1/2}$$

Thus, as the reverse bias voltage increases, the depletion region grows and the capacitance decreases. As discussed in the pulse processing chapter, a smaller capacitance is preferred for a good energy resolution. From the width of the depletion region, the active volume of the detector can be estimated.

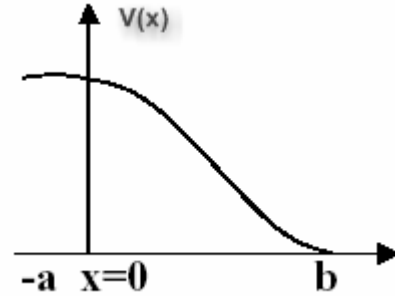


Fig. 7.12. Electric potential across the p-n junction.

7.5. Silicon diode detectors

A. Configurations

There are two well-known processes for manufacturing silicon diode detectors: ion implantation and surface-barrier technologies. The two processes are complementary in that each technique is best for manufacturing certain types of detectors. Fig. 7.13 shows simplified representations of the two manufacturing processes. Since the main application of the silicon diode detector is charged particle spectroscopy, minimizing the dead layer thickness is most important.

In the surface barrier type, thin metal layers are evaporated as doping impurities on the surface of the Si semiconductor after chemical etching while impurity ions are implanted by an accelerator in the ion implantation. The surface passivated with SiO_2 oxide keeps the leakage current much lower than in surface barrier detectors. Formation of the p-type layer through ion implantation also gives a very thin (down to ~ 34 nm) and uniform dead layer. Due to the relatively wide band gap of Si, silicon diode detectors can be operated at room temperature.

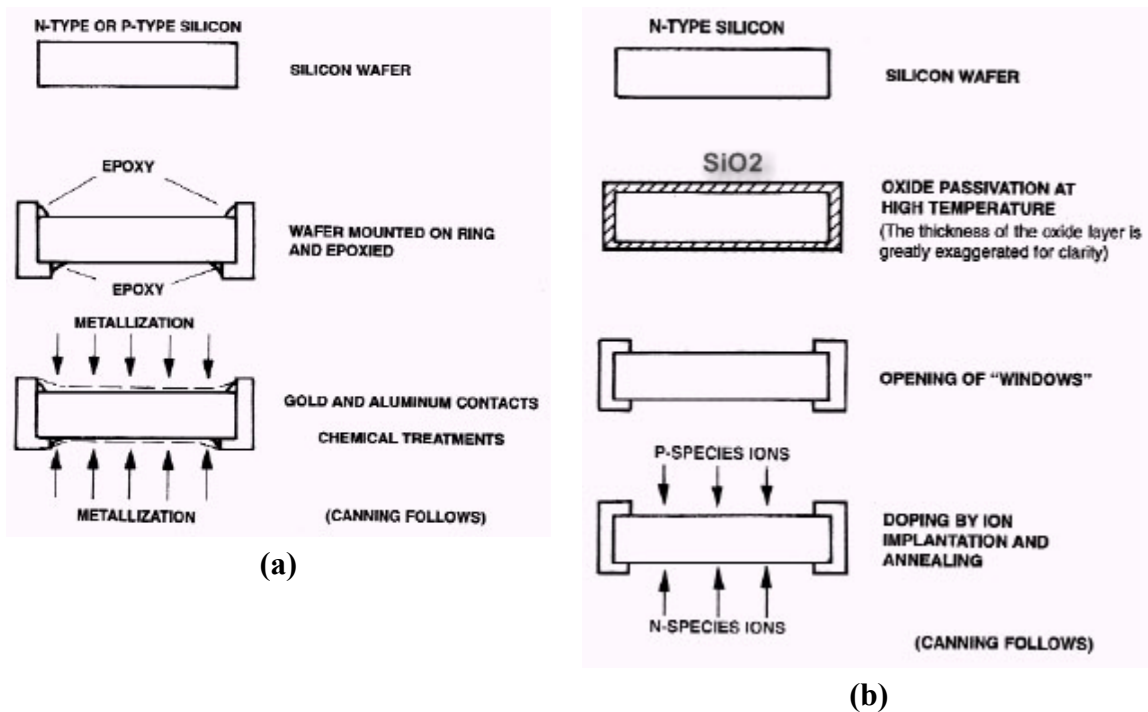


Fig. 7.13. Simplified diagrams of surface barrier (a) and ion-implanted processes (b).

B. Charged particle spectroscopy

Since their development in the early 1960s, silicon diode detectors have been used for applications related to charged particle spectroscopy. Sizes of detectors range from 1 to 5 cm^2 . A detector with a much bigger surface area can be fabricated as well. However, it will have a poor energy resolution due to its large capacitance. The depletion depth is limited up to ~ 1 mm. Considering the alpha particle range in Si as shown in Fig. 7.14,

this thickness is good enough for charged particle spectroscopy in most cases. Since the depletion depth is greater than the range of the incident ion, the response of the detector to a charged particle is very simple. For monoenergetic ions, only full-energy peaks are observed. An example of an alpha particle spectrum measured with a Si detector is shown in Fig. 7.15.

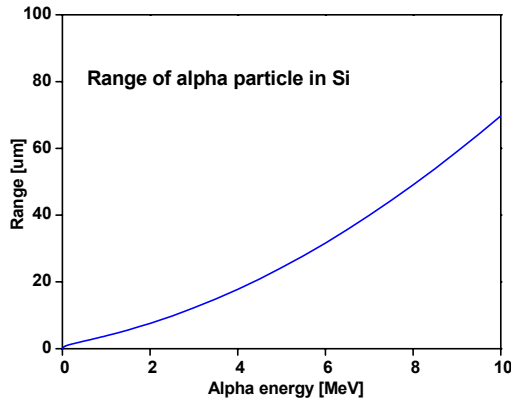


Fig. 7.14. Range of alpha particle in Si.

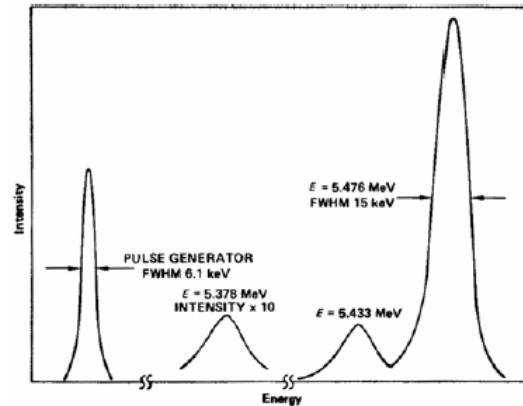


Fig. 7.15. ^{241}Am alpha spectrum.

Ion Beam Analysis (IBA) is one of the most important applications of the silicon diode detector. An energetic ion beam is useful for analyzing the compositional and structural characterization of a material surface. Depending on the charged particle interaction employed, IBA can be divided into Rutherford Backscattering Spectrometry (RBS), Elastic Recoil Detection (ERD), Particle Induced X-ray Emission (PIXE) or Gamma-ray Emission (PIGE). RBS and ERD are analytical methods involved with charged particle spectroscopy and described here.

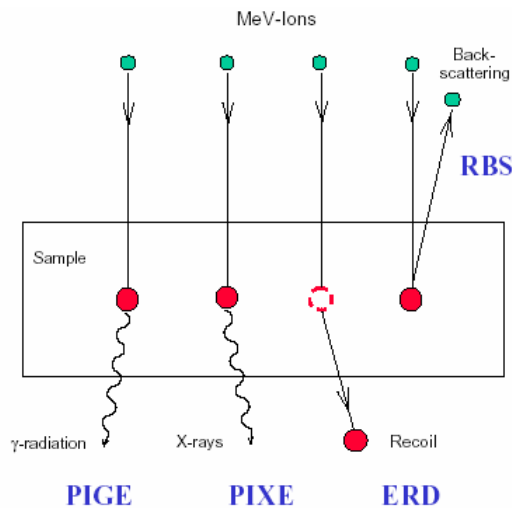


Fig. 7.16. Interaction between MeV ions and a material surface.

Rutherford Backscattering Spectrometry

RBS is the most frequently used ion beam analysis method. It relies on the fact that the energy of an elastically backscattered particle depends on the mass of the target atom (kinematic factor) and on the depth at which the scattering took place (energy loss on the way to and from the point of interaction). This make it possible to profile the elemental composition of the sample close to the surface. Practically, ⁴He ion beam with ~ 2 MeV backscattered to an angle close to 180° is suitable for most problems. The accessible depth for profiling is a couple of μm with a depth resolution of the order of 10 nm at the sample surface.

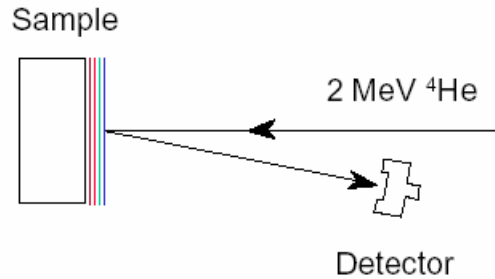


Fig. 7.17. Typical arrangement of RBS.

The identification of a certain atomic mass in the target is made via the kinematic factor k:

$$k = \frac{E'}{E} = \left(\frac{m \cos \theta + \sqrt{M^2 - m^2 \sin^2 \theta}}{m + M} \right)^2$$

where E is the energy of the incident ion with mass m, E' the energy of the backscattered projectile, M the mass of the target atom and θ the scattering angle. Thus, the backscattered energy is equivalent to a mass scale.

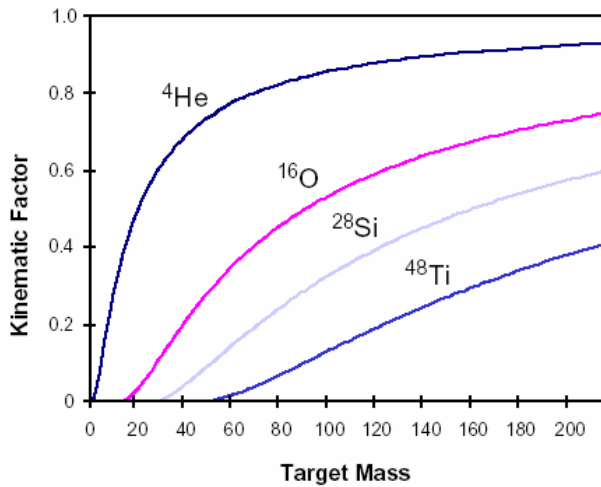


Fig. 7.18. Kinematic factor (at θ = 180°) as a function of target mass.

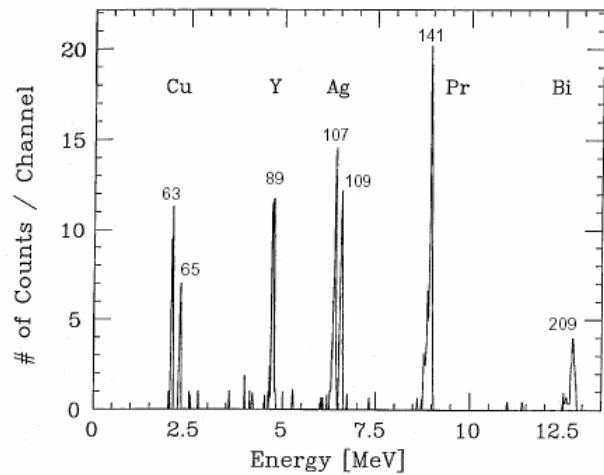
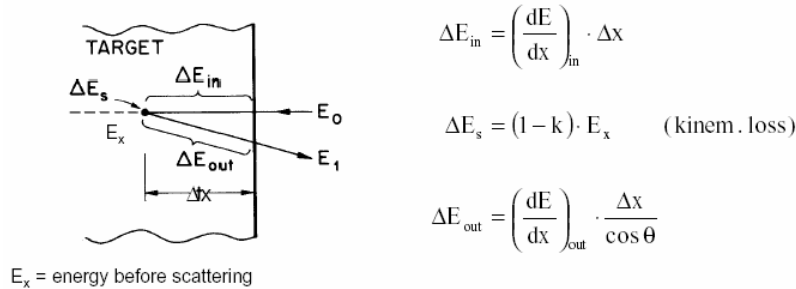


Fig. 7.19. RBS example demonstrating mass discrimination. Projectile: 25 MeV ³⁵Cl; target: thin layers of Cu, Y, Ag, Pr, Bi.

The energy loss of ions scattered at different depths is shown below. Ions undergo energy losses before and after scattering, and during the scattering.



$$\Delta E_{in} = \left(\frac{dE}{dx} \right)_{in} \cdot \Delta x$$

$$\Delta E_s = (1 - k) \cdot E_x \quad (\text{kinem. loss})$$

$$\Delta E_{out} = \left(\frac{dE}{dx} \right)_{out} \cdot \frac{\Delta x}{\cos \theta}$$

$$\text{Detected energy } E_1 = E_0 - \Delta E_{in} - \Delta E_s - \Delta E_{out}$$

$$\approx kE_0 - \underbrace{\left[\left(\frac{dE}{dx} \right)_{in} \cdot k + \left(\frac{dE}{dx} \right)_{out} \cdot \frac{1}{\cos \theta} \right]}_S \cdot x$$

Thus, the energy of ion coming out of the surface depends on both target element and scattering depth. An RBS spectrum is an overlay of the depth profiles of all individual atomic species present in the target material.

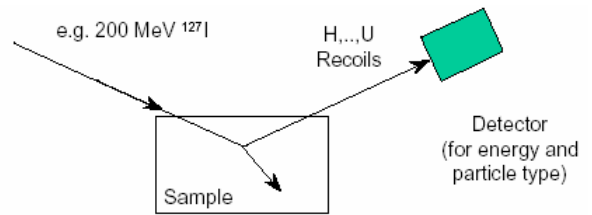
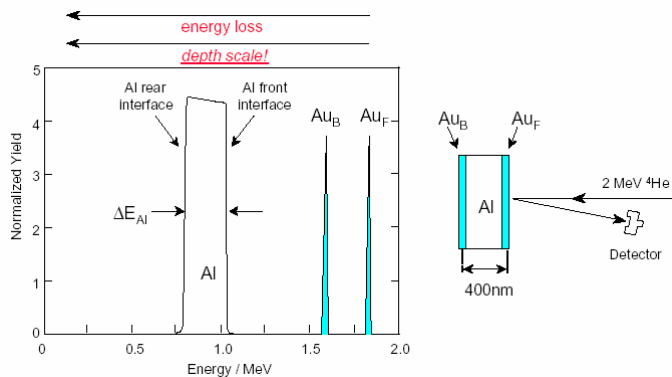


Fig.7. 21. Experimental setup for ERDA.

Fig. 7.20. Interpretation of the depth scale in RBS.

Elastic Recoil Detection

If light elements in heavy substrates or elements lighter than the incident beam particles have to be analyzed (e.g. hydrogen profiling) the recoiling target atoms can be detected in a grazing angle geometry. ERD is one of the few fully quantitative hydrogen profiling methods.

C. X-ray spectroscopy with silicon p-i-n diodes

Although lithium drifted Si or Hyperpure Ge are generally used for photon spectroscopy in the X-ray energy region, a simple Si p-i-n diode can be used as an alternative when LN₂ cooling is difficult to use. In this configuration, an intrinsic region is provided in the middle to reduce the leakage current further. The mean free path of a photon at 10 keV is ~ 0.1 mm as shown in Fig. 7.22, so that 1 mm thickness is adequate for X-ray detection.

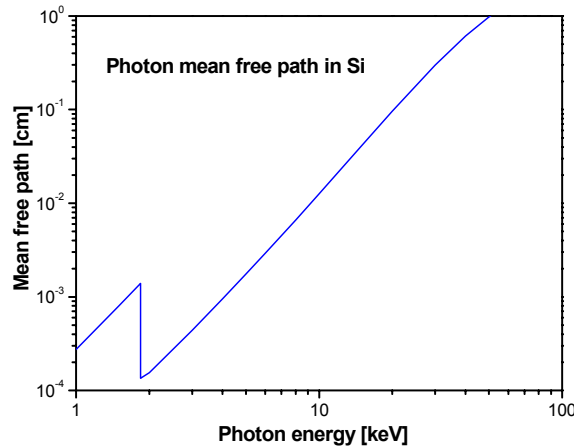


Fig. 7.22. Photon mean free path in Si.

The relatively small number of electron-hole pairs created by a soft X-ray photon requires the noise of the detector to be further reduced. Cooling to ~ - 30 °C using a compact thermoelectric cooler has technically been developed. Fig. 7.24 shows the energy dependence of the intrinsic peak efficiency.

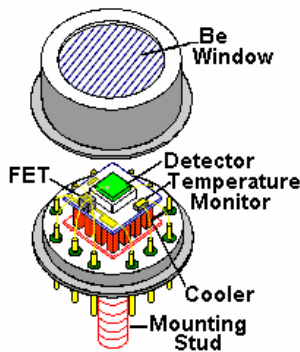


Fig. 7.23. Si p-i-n diode detector for X-ray spectroscopy.

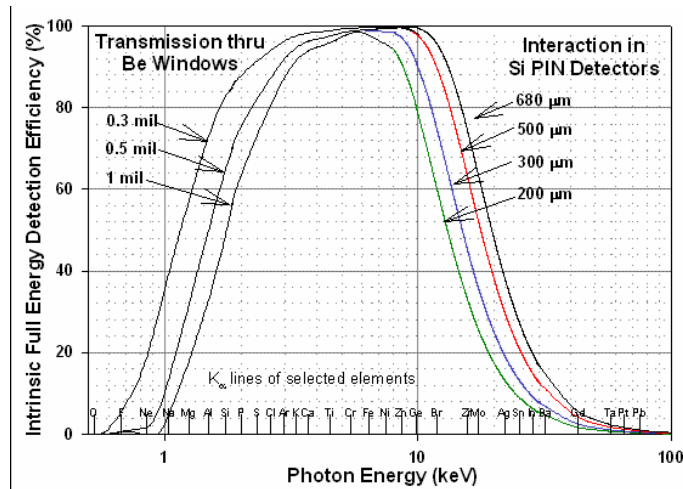


Fig. 7. 24. Peak efficiencies of Si p-i-n and lithium drifted Si detectors.

References

1. G.F. Knoll, Radiation Detection and Measurement - 3rd edition (Chapter 11), John Wiley & Sons, 1999.
2. Introduction to Charged-Particle Detectors, ORTEC, *URL: <http://www.ortec-online.com/>*.
3. R.H. Redus, A.C. Huber, J.A. Pantazis, Nucl. Instr. and Meth. A 458 (2001) 214.